International Journal of Hybrid Information Technology
Vol. 9, No.11 (2016), pp. 199-206
http://dx.doi.org/10.14257/ijhit.2016.9.11.17

MRI Segmentation of a Prostate Based on Distance Regularized Level Set Evolution with a Priori Shape

Jingchun Peng[1, 2], Yongde Zhang[1*], Gang Liu[1], Jingang Jiang[1] and Yanjiang Zhao[1]

[1]*Intelligent Machine Institute, Harbin University of Science and Technology, China*
[2]*Harbin Huade University, China*
[*]*zhangyd@hrbust.edu.cn, pjc8996@126.com*

Abstract

Prostate segmentation from MRI is a necessary first step and plays a key role in different stages of clinical decision making process. In this paper, we propose a MR T1 Image segmentation method of the prostate based on distance regularized level set evolution with a deformable shape prior. To smooth the prostate image to reduce the noise, we introduce a prostate image with Gaussian kernel and get an edge indicator. To avoid the leakage induced on account of prostate boundaries missing, or blending with surrounding tissues, we introduce priori shape information to construct an energy function with a distance regularization term and an external shape energy term containing the edge indicator and minimize it by solving the gradient flow which can be implemented with a finite difference scheme. To verify the MRI segmentation method of a prostate presented in this paper, we utilize the optimal value of parameters λ , μ , α *and* ε *in the distance regularized level set evolution model and the deformable shape prior of prostate to segment a part of images from normal prostate, benign hyperplasia prostate and cancer prostate. The experiment results show that the MRI segmentation method of prostate presented in this paper is effective for different situation of different patients.*

Keywords*: Image segmentation, Prostate, Magnetic resonance imaging, Level set, Active contours model, priori shape*

1. Preface

Prostate cancer is the most common malignant tumor in male. The clinic treatment shows that if prostate cancer is detected early, men have a higher survival rate. Therefore, there is a high value on prostate cancer diagnosis and treatment. Magnetic resonance imaging (MRI) has higher accuracy in the detection of prostate cancer and is considered to be the most effective imaging techniques at present [1]. Prostate segmentation from MRI is a necessary first step and plays a key role in different stages of clinical decision making process [2-4]. However, manual segmentation of a prostate is a laborious and time consuming work and different physician is easy to make the different segmentation results. So, accurate computerized prostate segmentation based on MRI is extremely useful.

The Active Shape Model is a popular segmentation method. M. Yang and X. Li [5] proposed a distinctive image appearance descriptor that was incorporated in the active shape model to segment the prostate from T2W MRI. R. Toth and A. Madabhushi [6] presented a novel active appearance models methodology that utilized the level set to realize the most accurate segmentation. Level set as a more effective method of the prostate segmentation based on MRI has a certain advantage. However, the level set function (LSF) typically develops irregularities during its evolution, which cause numerical errors and eventually destroy the stability of the level set evolution. To overcome these problems, the reinitialization is performed by periodically stopping the

ISSN: 1738-9968 IJHIT

evolution and reshaping the degraded LSF as a signed distance function. However, when and how the reinitialization should be performed introduces more serious problems and affects the accuracy in an undesirable way. Chunming Li[7]proposed an idea of distance regularized level set evolution that needn't reinitialization and avoided the numerical errors. In MR images, the prostate and surrounding tissues have overlapping intensity and texture, and prostate boundaries may be missing, or blended with surrounding tissues. Under such conditions, using some priori shape information could help the segmentation algorithm perform better [8-11]. This paper will improve the distance regularized level set evolution method by newly adding a shape energy term in the energy function which ensures the convergence of level set function during evolution and realizes effectively the segmentation of MR T1 image for different situation of different prostate patients.

2. Priori Shape Modeling

A prostate locates at the base of pelvic cavity, whose shape likes an obsequent chestnut. The top of prostate is wider and named prostate bottom. A prostate has transverse diameter 4 cm, longitudinal diameter 3 cm and before and after diameter 2 cm. It is a bladder at the top of a prostate, a urethra at the bottom of a prostate, a pubic bone in front of a prostate and a rectum at rear of a prostate. The side view of prostate is shown in Figure 1 and the rear view of prostate is shown in Figure 2. The right and left of a prostate are fixed by many ligaments and fascia. The seminal vesicle is at the right and left side behind the prostate. A urethra runs through the prostate from the front 1/3 of the prostate bottom, ejaculatory duct runs though the prostate from top to bottom, and its openings is in the middle fossae of the prostate.

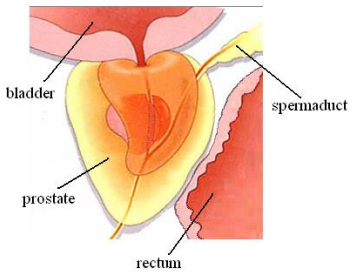

Figure 1. The Prostate Viewed From the Side

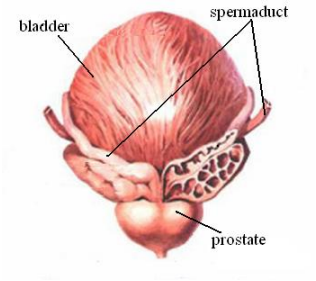

Figure 2. The Prostate Viewed From the Rear

We may assume that the prostate is a flexible ellipsoid and construct a deformable ellipse model [12] to describe the prostate cross-section shape.

The basic ellipse parametric function is as follows:

$$\begin{cases} x = a_x \cos\alpha \\ y = a_y \sin\alpha \end{cases} \qquad \alpha \in [-\pi, \pi] \tag{1}$$

where a_x is the length of the x semi axis, a_y is the length of the y semi axis.

In Figure 3(c), the shape of prostate mainly changes along the y axis. So, we may get a parametric equation of deformable ellipse $\psi(x_d, y_d)$ by transforming the basic ellipse function along the y axis, as shown in follows:

$$\begin{cases} x_d = (a_y / b_y - a_y \sin\alpha - y_c)\sin\beta \\ y_d = a_y / b_y - (a_y / b_y - a_y \sin\alpha - y_c)\cos\beta \end{cases} \qquad \alpha \in [-\pi, \pi] \tag{2}$$

where

$$\beta = \frac{[t_y(a_y \sin\alpha + y_c)/a_y + 1]a_x \cos\alpha}{a_y / b_y - a_y \sin\alpha - y_c} \tag{3}$$

In the above equations, y_c is the center coordinate of an ellipse, $t_y \in [-1,1]$ is the linear tapering value along y axis, $b_y \in [-1,0) \cup (0,1]$ is the circular bending value along y axis. In fact, we may change different set of (a_x, a_y, y_c, t_y, b_y) to model a large variety of natural shapes. To fit a variety of prostate shapes well, we select data sets of deformable ellipse models with varying quality of fit, as shown in Figure 3. Figure 4 shows the deformable ellipse models which describe the shape of different slice of a normal prostate.

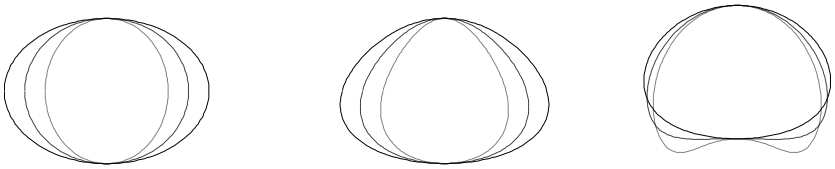

(a) a_x=25,20,15 a_y=15 (b) t_y=-0.2,-0.25,-0.3 (c) b_y=-0.1,-0.3,-0.5

Figure 3. Deformable Ellipses of Varying Global Shape Parameters Fitting Prostate Shapes. The Solid, Dashed and Dotted Curves are corresponding to the First, Second and Third Parameters Respectively

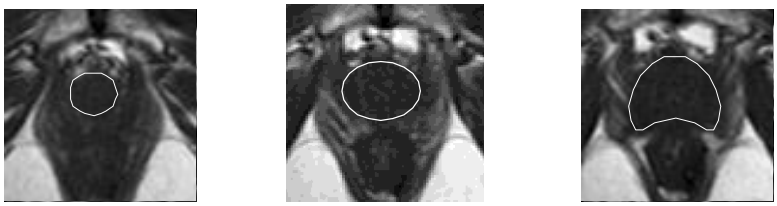

(a) the 7th slice (b) the 8th slice (c) the 9th slice

Figure 4. The Deformable Ellipse Models Describing the Shape of Different Slice of a Normal Prostate

3. Segmentation of the Prostate

When the prostate and its surrounding tissues have overlapping intensity and texture, the prostate boundaries may be missing, or blended with its surrounding tissues. Under such conditions, the traditional distance regularized level set evolution method is difficult to get a satisfied segmentation result. So this section will add a new shape energy term in the energy function, which can ensure the convergence of level set function during evolution and help the segmentation algorithm perform better. We call this method an improved distance regularized level set evolution with a priori shape.

Firstly, to reduce an image noise, we smooth the initial image using convolution operating. Let I be the prostate image, an edge indicator function g is defined by

$$g = \frac{1}{1+\left|\nabla G_\sigma * I\right|^2} \tag{4}$$

where G_σ is a Gaussian kernel with a standard deviation σ. This function g usually takes smaller values at prostate boundaries than at other locations.

For a LSF $\phi : \Omega \to \Re$, we define an energy function $\varepsilon(\phi)$ with a priori shape term by

$$\varepsilon(\phi) = \mu \boldsymbol{R}_p(\phi) + \lambda \boldsymbol{E}_{1g}(\phi) + \alpha \boldsymbol{E}_{2g}(\phi) + \beta \boldsymbol{E}_s(\phi, \psi) \tag{5}$$

where $\boldsymbol{R}_p(\phi)$ is the level set regularization term, μ is a constant, $\lambda > 0$, $\alpha \in \Re$ and $\beta < 0$ respectively are the coefficients of the energy functions $\boldsymbol{E}_{1g}(\phi)$, $\boldsymbol{E}_{2g}(\phi)$ and $\boldsymbol{E}_s(\phi, \psi)$, which are defined by

$$\boldsymbol{E}_{1g}(\phi) = \int_{\Omega} g\delta(\phi)|\nabla\phi|\,d\mathbf{x} \tag{6}$$

and

$$\boldsymbol{E}_{2g}(\phi) = \int_{\Omega} gH(-\phi)d\mathbf{x} \tag{7}$$

and

$$\boldsymbol{E}_{s}(\phi,\psi) = \int_{\Omega}\left(H(\phi)-H(\psi)\right)^{2}d\mathbf{x} \tag{8}$$

where δ and H are the Dirac delta function and the Heaviside function, respectively.

With the Dirac delta function δ , the energy $\boldsymbol{E}_{1g}(\phi)$ computes the line integral of the function along the zero level contour of ϕ . The energy function $\boldsymbol{E}_{2g}(\phi)$ computes a weighted area of the region $\Omega_{\phi}^{-} = \{\mathbf{x}:\phi(\mathbf{x})<0\}$. The shape energy function $\boldsymbol{E}_{s}(\phi,\psi)$ computes the shape difference between the current zero level set ϕ and the priori shape ψ defined in (2).

In practice, the Dirac delta function δ and Heaviside function H are approximated by the following smooth functions δ_{ε} and H_{ε} as in many level set methods defined by

$$\delta_{\varepsilon} = \begin{cases} \dfrac{1}{2\varepsilon}\left[1+\sin\left(\dfrac{\pi x}{\varepsilon}\right)\right], & |x| \le \varepsilon \\ 0, & |x| > \varepsilon \end{cases} \tag{9}$$

and

$$H_{\varepsilon} = \begin{cases} \dfrac{1}{2}\left[1+\dfrac{x}{\varepsilon}+\dfrac{1}{\pi}\cos\left(\dfrac{\pi x}{\varepsilon}\right)\right], & |x| \le \varepsilon \\ 0, & x > \varepsilon \\ 0, & x < -\varepsilon \end{cases} \tag{10}$$

Note that δ_{ε} is the derivative of H_{ε}, *i.e.*, $H_{\varepsilon}' = \delta_{\varepsilon}$.

With the Dirac delta function δ and Heaviside function H in (6), (7) and (8) being replaced by δ_{ε} and H_{ε}, the energy function $\varepsilon_{\varepsilon}(\phi)$ is then approximated by

$$\boldsymbol{\varepsilon}_{\varepsilon}(\phi) = \mu\int_{\Omega} p(|\nabla\phi|)d\mathrm{x} + \lambda\int_{\Omega} g\delta_{\varepsilon}(\phi)|\nabla\phi|\,d\mathrm{x} + \alpha\int_{\Omega} gH_{\varepsilon}(-\phi)d\mathrm{x} + \beta\int_{\Omega}\left(H(\phi)-H(\psi)\right)^{2}d\mathrm{x} \tag{11}$$

This energy function (11) can be minimized by solving the following gradient flow:

$$\frac{\partial\phi}{\partial t} = \mu\,\mathrm{div}\left(d_{p}(|\nabla\phi|)\nabla\phi\right) + \lambda\delta_{\varepsilon}(\phi)\,\mathrm{div}\left(\mathrm{g}\frac{\nabla\phi}{|\nabla\phi|}\right) + \alpha g\delta_{\varepsilon}(\phi) + 2\beta\left(H(\phi)-H(\psi)\right) \tag{12}$$

given an initial LSF $\phi(\mathrm{x},0) = \phi_{0}(\mathrm{x})$. The first term on the right hand side in (12) is associated with the distance regularization energy $\boldsymbol{R}_{p}(\phi)$, while the second and third terms are associated with the energy terms $\boldsymbol{E}_{1g}(\phi)$ and $\boldsymbol{E}_{2g}(\phi)$, respectively, the fourth term is associated with the shape prior energy $\boldsymbol{E}_{s}(\phi,\psi)$.

The distance regularized level set evolution with a priori shape in (12) can be implemented with a simple finite difference scheme as follows. The temporal partial derivative $\partial\phi/\partial t$ is approximated by the forward difference. The time dependent LSF $\phi(x,y,t)$ is given in discretized form $\phi_{i,j}^{k}$ with spatial index (i,j) and temporal index k. Then, the level set evolution equation is discretized as the following finite difference equation

$$\phi_{i,j}^{k+1} = \phi_{i,j}^{k} + \Delta tL\left(\phi_{i,j}^{k}\right), \qquad k = 0,1,2... \tag{13}$$

where $L\left(\phi_{i,j}^{k}\right)$ is the approximation of the right hand side in the evolution equations. The equation (13) is an iteration process used in the numerical implementation of the distance regularized level set evolution with a priori shape so as to realize the segmentation of prostate.

4. Experiment Results

The magnetic resonance images of prostate used in this section is offered by Harbin Humor Hospital and come to 30 images from 10 cases including normal cases, benign hyperplasia cases and cancer cases. In the improved distance regularized level set evolution model (12), there are parameters λ , μ , α ε and β , which can be generally fixed for most of applications. We have discussed the effects of these parameters on the segmentation of prostate by respectively changing parameter value for one image. To verify the MRI segmentation method of a prostate present in this paper, we select λ=2 , α=−6 , ε=1.5 and μ=0.2 to segment the eighth, ninth and tenth image from one normal prostate. Figure 5 shows the MRI segmentation results of the 8th slice of one normal prostate. Figure 5 (a) shows the deformable ellipse, which best fits the prostate can roughly model the prostate shape, and we define the parameters t_y=0.3 , b_y=0.45 . Figure 5(b) is the segmentation result obtained by the distance regularized level set evolution without a priori shape. From Figure 5(b), we can see the boundary between prostate and rectum is very weak, certain surrounding tissues that are not part of the prostate are segmented as the prostate. Figure 5(c) illustrates the final result obtained by the distance regularized level set evolution with a priori shape and the shape coefficient is defined β=-0.2 . From the Figure 5(c), we may clearly see that the segmentation algorithm with a prior shape converges well to the prostate border, and then avoids effect of a weak edge.

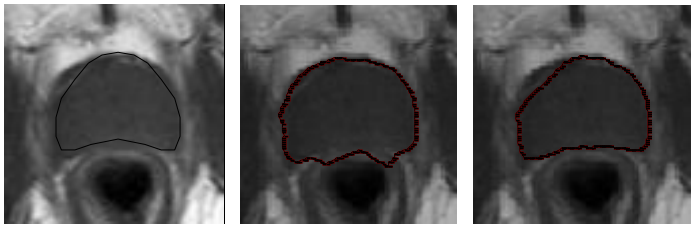

(a) (b) (c)

Figure 5. MRI Segmentation Results of the 8th Slice. (A) The Deformable Ellipse Fitting the Prostate, (B) The Segmentation Result Obtained Without Priori Shape, (C) the Final Segmentation Result with Priori Shape

To further prove the effectiveness and accuracy of the segmentation method presented in the paper, we select a part of images from normal prostate, benign hyperplasia prostate and cancer prostate as samples to have an experimental study and compare the result of the segmentation method and manual segmentation. Figure 6 shows the comparison results of the segmentation. From these figures, it can be seen easily that the segmentation results (white lines) using the algorithm present in this paper are similar to the manual segmentation results (black lines). We can conclude easily that the MRI segmentation method of prostate presented is effective and accurate for different situation of different prostate patients.

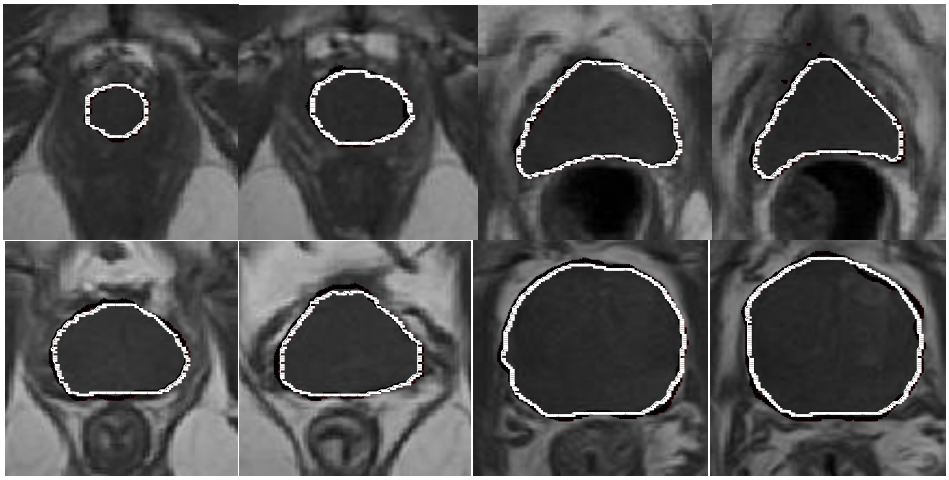

Figure 6. Final Results of Computerized Segmentation and Manual Segmentation for Eight Samples

5. Conclusion

A MR T1 image segmentation method of a prostate based on distance regularized level set evolution with a priori shape is presented in this paper. We select the optimal value of parameters λ, μ, α and ε in the distance regularized level set evolution model to have an experimental study on the segmentation of a prostate with a priori shape. The experimental result shows that the method with a priori shape can avoid the leakage induced on account of prostate boundaries missing and blending with surrounding tissues. To verify the effectiveness of the MR T1 image segmentation method presented in this paper of a prostate, we segment a part of images from normal prostate, benign hyperplasia prostate and cancer prostate. The results show that the method with a priori shape is effective and accurate for different situation of different prostate patients.

Acknowledgements

This research was supported by the National Natural Science Foundation of China (Grant No 51305107), Research Fund for the Doctoral Program of Higher Education of China (Grant No. 20122303110006), Natural Science Foundation of Heilongjiang Province of China (Grant Nos E2015059, E201448).

References

[1] J. C. Weinreb and F. V. Coakley, "MR Imaging and MR Spectroscopic Imaging of Prostate Cancer Prior to Radical Prostatectomy: a Prospective Multi-Institutional Clinic Opathological Study", Presented at RSNA, Chicago, vol. IL, **(2006)**.
[2] G. Litjens, R. Toth and W. Van De Ven, "Evaluation of prostate segmentation algorithms for MRI: the promise12 challenge", Medical Image Analysis, no. 18, **(2014)**, pp. 359–373.
[3] P.C. Vos, J.O. Barentsz, N. Karssemeijer and H.J. Huisman, "Automatic computer aided detection of prostate cancer based on multiparametric magnetic resonance image analysis", Phys. Med. Biol, no. 57, **(2012)**, pp. 1527–1542.
[4] P. Tiwari, J. Kurhanewicz and A. Madabhushi, "Multi-kernel graph embedding for detection, gleason grading of prostate cancer via MRI/mrs", Med. Image Anal, no. 17, **(2013)**, pp. 219–235.
[5] M. Yang and X. Li, "Prostate segmentation in MR images using discriminant boundary features", IEEE Transactions on Biomedical Engineering, pp. 60, no. 2, **(2013)**, pp. 479.
[6] R. Toth and A. Madabhushi, "Multi-feature landmark-free active appearance models: application to prostate MRI segmentation", IEEE Trans. Med. Imag., **(2012)**, pp. 1638–1650.

[7] C. Li, C. Xu, C. Gui and M. D. Fox, "Distance regularized level set evolution and its application to image segmentation", IEEE TRANSACTIONS ON IMAGE PROCESSING, vol. 12, no. 19, **(2010)**, pp. 3243-3254.
[8] X. Liu, M. A. Haider and I. Samil Yetik, "Unsupervised 3D prostate segmentation based on diffusion-weighted imaging MRI using active contour models with a shape prior", Hindawi Publishing Corporation Journal of Electrical and Computer Engineering, **(2011)**, pp. 1-11.
[9] X. Wei, "Automatic 3D prostate MR image segmentation using graph cuts and level sets with shape prior", Advances in Multimedia Information Processing – PCM 2013, Lecture Notes in Computer Science, **(2013)**, pp. 211-220.
[10] F. Derraz, L. Peyrodie and A. Taleb-Ahmed, "Interactive binary active contours for prostate contour delineation", Proceedings of the 2012 IEEE 12th International Conference on Bioinformatics & Bioengineering (BIBE), Larnaca, Cyprus, **(2012)**, pp. 494-499.
[11] A. Skalski, J. Lagwa and P. Kedzierawski, "Automatic Prostate Segmentation in MR images Based on 3D Active Contours with Shape Constraints", Signal Processing Algorithms, Architectures, Arrangements, And Applications, Spa 2013, Poland, **(2013)**, pp. 246-249.
[12] L. Gong,S.D.Pathak, D. R. Haynor, P. S.Cho and Y. Kim, "Parametric Shape Modeling Using Deformable Superellipses for Prostate Segmentation", IEEE Transactions On Medical Imaging, vol. 3, no. 23, **(2004)**, pp. 340-349.

